Investigation of the thermal conductivities across metal-insulator transition in polycrystalline VO_2

CHEN JiKun[1,2], LIU XinLing[2], YUAN Xun[2], ZHANG YuLiang[1], GAO YanFeng[2], ZHOU YanFei[2], LIU RuiHeng[2], CHEN LiDong[2*] & CHEN NuoFu[1*]

[1] *School of Renewable Energy, North China Electric Power University, Beijing 102206, China;*
[2] *CAS Key laboratory of Materials for Energy Conversion, Shanghai Institute of Ceramics, Chinese Academy of Sciences, Shanghai 200050, China*

Previous reports about the thermal conductivities of VO_2 showed various temperature dependences across metal-insulator transition (MIT) temperature. In this work, polycrystalline VO_2 samples were fabricated by spark plasma sintering of VO_2 powder. Temperature dependences of their thermal conductivities were investigated using laser flash technique, and the thermal conductivity showed a significant decrease trend from metal-phase to insulator phase. Electrical transport properties were investigated to confirm both carrier and lattice contribution to the thermal conductivity. It is found that the lattice thermal conductivity decreased significantly across MIT point, which may be caused by soft phonon mode in metal phase of VO_2.

thermal conductivity, phase transformation, VO_2

The metal-insulator transition (MIT) in vanadium dioxide (VO_2) has received considerable attentions due to its potential applications in optical waveguides and high-speed electronics [1,2]. At the MIT temperature around 68°C, VO_2 exhibits a phase transition from high-temperature metallic behavior to low-temperature insulating or semi-conductive behavior [3]. Along with this transition, the optical, magnetic and electrical transport properties of vanadium dioxide change dramatically within a narrow temperature interval, which have received intensive investigation in the last decade [4–6]. However, the thermophysical properties of VO_2, such as thermal conductivity, near the MIT temperature have been less concerned. As to further satisfy the development of VO_2 based high speed energy switch devices, investigation and comprehension of the thermal transportation properties of VO_2 are still needed [7].

Previous reports about the thermal conductivity of VO_2 showed various values and temperature dependences across MIT temperature [8–14]. Berglund et al. [8] reported that the thermal conductivity of bulk VO_2 sample changed little when passing through the transition point, whereas Andreev et al. [9] reported a marked decrease from insulating phase to metallic phase. Recently, Oh et al. [10] applied a novel method to the thermal conductivity measurement of VO_2 thin films and found that the thermal conductivity would increase by 60% in the metallic phase, which could be comprehended as the contribution of the increased electrical conductivity assuming that the lattice contribution of thermal conductivity remains the same before and after the MIT point. The variety of these results makes it necessary to investigate more about the thermal conductivity of VO_2. In this work, polycrystalline VO_2 samples were fabricated by spark plasma sintering (SPS) using micro-scaled VO_2 powder. The thermal conductivity of as-produced VO_2 sample near the MIT temperature was measured using laser flash method, and the temperature dependence of lattice thermal

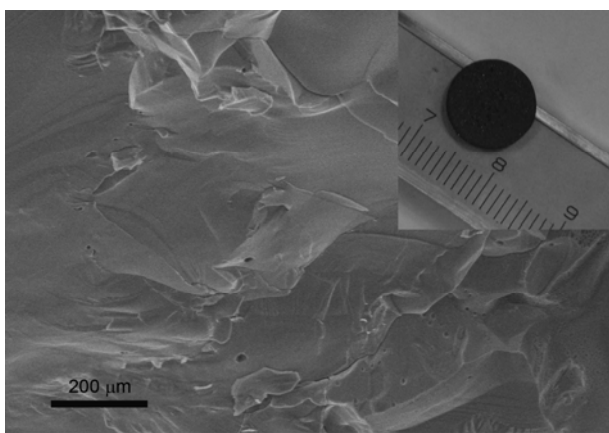*Corresponding authors (email: nfchen@ncepu.edu.cn; chenlidong@mail.sic.ac.cn)
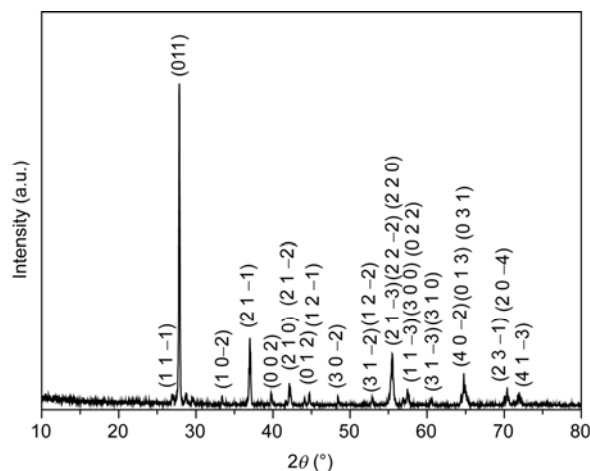
conductivity was also investigated.

1 Experimental

VO$_2$ powder used for SPS was fabricated using the method reported by Peng et al. [11]. The obtained VO$_2$ powder was sintered into a dense polycrystalline solid using the spark plasma sintering technique (SPS-2040) at 900°C under 20 MPa for 10 min in a graphite die. Relatively high-density samples (>98% of the theoretical density) with diameter of 10 mm and thickness of 1.5 mm were obtained in the present study. X-ray diffraction data was collected on a diffractometer (Rigaku, RINT2000) with CuKα radiation at room temperature to examine the phase purity and structure. The measurement of thermal diffusivity (λ) was carried out using the laser flash method in a flowing Ar atmosphere (Netzsch LFA 427), and the measurement was performed in the temperature range of 20–150°C. The sample of VO$_2$ was sprayed with graphite in each surface when carrying out the thermal diffusivity measurement. The heat capacity C_p of the sample after SPS treatment was measured by differential scanning calorimetry (PE DSC-2C) in the temperature range of 25–150°C. Thermal conductivity (κ) was calculated from the relationship $\kappa = \rho\lambda C_p$, where λ is the thermal diffusivity coefficient, C_p is the heat capacity and ρ is the density of the material. Samples used for electrical transport measurements were cut into rectangular bars with the approximate dimensions of 1 mm × 2 mm × 10 mm, and the measurement of electrical conductivity and Seebeck coefficient were carried out using ZEM-3 (ULVAC-RLKO) under the temperature range of 20–150°C.

2 Results and discussion

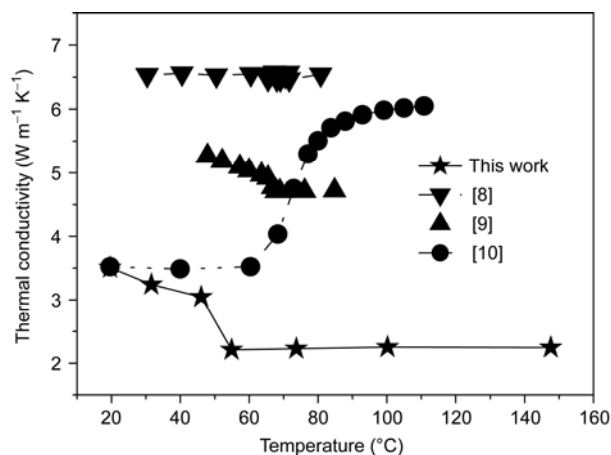Figures 1 and 2 show the SEM image of fractured surface

Figure 2   XRD pattern of as-SPSed VO$_2$ (measured at room temperature), with main peaks indexed as monoclinic phase.

and the XRD pattern of the VO$_2$ sample after SPS, respectively. During the SPS process, the pulsed DC current directly passes through the graphite die and the powder compact, which generates the heat internally and enhances the densification of the sample. Besides, the decreased sintering time in SPS process maintains the origin chemical state of VO$_2$ that is sensitive to the atmosphere in high temperature. It can be seen that the as-produced VO$_2$ sample possesses polycrystalline structure with monoclinic structure, which accords with the low-temperature phase of VO$_2$. The grain size of the sample was around tens of micrometers, and the density of the as-sintered sample reached 4.62 g cm^{-3}, compared with the theoretical density of 4.65 g cm^{-3}.

Thermal conductivity of as-produced VO$_2$ sample is shown in Figure 3, together with those reported previously. In this work, thermal conductivity of the polycrystalline VO$_2$ sample is about 3.5 W m^{-1} K^{-1} in the insulating phase, which stood at a similar magnitude with the recent result obtained by Oh et al. [10] in VO$_2$ thin films. As for higher

Figure 1   SEM image of the fracture surface morphology of the VO$_2$ sample after SPS, with inset showing the photo of as-SPSed VO$_2$ sample.

Figure 3   Thermal conductivity of the as-sintered VO$_2$ sample, compared with results from previous reports.

temperature metallic phase, the thermal conductivity showed a significant decrease about 35% that accords with the report from Andreev [9]. The thermal conductivity was measured during a heating process. To testify the reversibility of this change, the thermal conductivity was measured again when temperature dropped to around 20°C, and the thermal conductivity returned to the same magnitude of the low temperature phase.

The as-measured thermal conductivity κ is a sum of two contributions: lattice part κ_L and carrier part κ_c. κ_c can be estimated by the Wiedemann-Franz law as $\kappa_c = L_0 \sigma T$, where L_0 is the Lorenz number (2.45×10^{-8} V^2 K^{-2}). That the temperature dependence of thermal conductivity across the MIT point is different in this work compared with that in Oh's should be attributed to the different carrier contribution of thermal conductivity. In order to further calculate the lattice contribution to thermal conductivity, temperature dependence of the electrical transport properties of the samples was also measured. As shown in Figure 4, the negative Seebeck coefficient through the whole temperature range indicates that the main carrier is electron in both phases. Around 65°C, the electrical conductivity of the sample increased about one magnitude within a narrow temperature range, while the Seebeck coefficient decreased significantly, which indicates that the carrier concentration increased significantly by the phase transition from insulating phase to metallic phase. However, the enhancement of the electrical conductivity in our sample is not as large as what were reported in single crystalline or thin film VO$_2$ samples. The metallic phase of the VO$_2$ sample showed semiconducting character, since the electrical conductivity was found to increase with temperature in the present sample. This indicates that there may be localized states or electrons, which could be caused by defects like grain boundaries and pores. By heat excitation, these localized electrons would become carriers and contribute to the electrical conductivity. What also needs to mention is that the phase transition temperature shown in thermal conductivity measurement was prior to that measured in the electrical conductivity. This is mainly caused by the used laser flashing, which would generate extra heat to cause a temperature rise of 2–5°C of the sample compared with the background temperature, and will induce the phase transition when background temperature was close to the MIT point.

The calculated lattice thermal conductivity of as-produced VO$_2$ sample is shown in the downside picture in Figure 4. The lower lattice thermal conductivity κ_L in the metallic phase of VO$_2$ was possibly caused by the soft phonon mode in the high temperature phase, which has been proved directly in the XRD scatting experiment [12]. On the other hand, the high temperature phase of VO$_2$ has lower acoustic velocity according to dispersion relationship, which has been observed by measuring Rayleigh velocity before and after phase transition [13,14]. The significant decrease of lattice thermal conductivity κ_L counts for the negative temperature dependence of the total thermal conductivity across the MIT point, since the carrier contribution κ_c is low in our samples.

3　Conclusion

In summary, polycrystalline VO$_2$ samples with high relative density were fabricated by spark plasma sintering (SPS) using micrometer-sized VO$_2$ powder. The temperature dependence of the thermal conductivity across MIT point was investigated using standard laser-flash method. For our samples, the total thermal conductivity showed 30% decrease from low-temperature insulating phase to high temperature metallic phase. This negative temperature dependence of thermal conductivity across MIT point is caused by the decrease of lattice thermal conductivity across the phase transition, since the carrier contribution of thermal conductivity is low. The different variation trends of thermal conductivity of VO$_2$ across MIT point in previous reports might be caused by the difference in carrier contribution to the thermal conductivity, which is sensitive to the structure and defects of the samples.
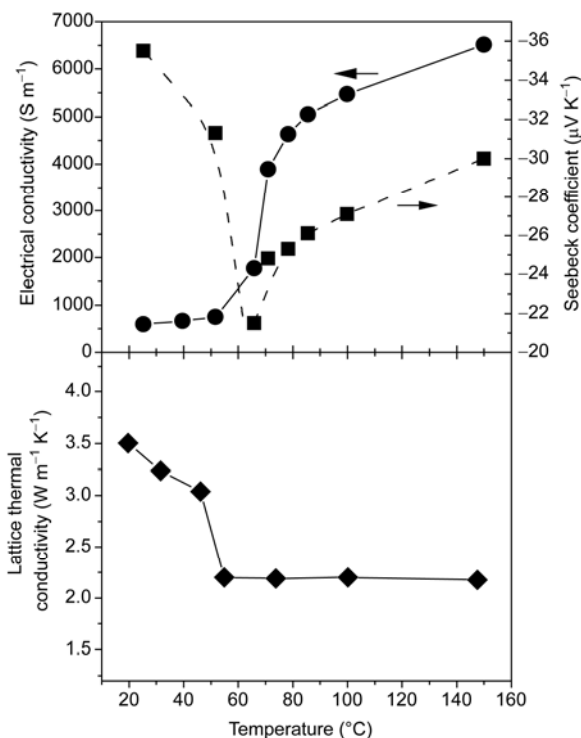
Figure 4 Electrical conductivity, Seebeck coefficient and lattice thermal conductivity of the VO$_2$ sample in the temperature range of 20–150°C. The solid line with round point shows the electrical conductivity, while the dash line with square point shows the Seebeck coefficient.

1   Lee M J, Park Y. Two series oxide resistors applicable to high speed and high density nonvolatile memory. Adv Mater, 2007, 19: 3919–3923
2   Rini M, Hao Z. Optical switching in VO_2 films by below-gap excitation. Appl Phys Lett, 2008, 92: 181904
3   Morin J. Oxides which show a metal-to-insulator transition at the Neel temperature. Phys Rev Lett, 1959, 3: 34–36
4   Donev E U, Lopez R. Confocal Raman microscopy across the metal-insulator transition of single vanadium dioxide nanoparticles. Nano Lett, 2009, 9: 702–706
5   Qazilbash M M, Brehm M. Infrared spectroscopy and nano-imaging of the insulator-to-metal transition in vanadium dioxide. Phys Rev B, 2009, 79: 075107
6   Lee M H. Thermochromic glazing of windows with better luminous solar transmittance. Sol Energy Mater Sol Cells, 2002, 71: 537–540
7   Chang C W, Okawa D. Solid-state thermal rectifier. Science, 2006, 314: 1121–1124
8   Berglund C N, Guggenheim H J. Electronic properties of VO_2 near semiconductor-metal transition. Phys Rev B, 1969, 185: 1022–1033
9   Andreev V N, Chudnovskii F A. Thermal conductivity of VO_2, V_3O_5, and V_2O_3. Phys Status Solidi (a), 1978, 48: K153–K156
10 Oh D W, Ko C Y. Thermal conductivity and dynamic heat capacity across the metal-insulator transition in thin film VO_2. Appl Phys Lett, 2010, 96: 151906
11 Peng Z F, Jiang W. Synthesis and electrical properties of tungsten-doped vanadium dioxide nanopowders by thermolysis. J Phys Chem C, 2007, 111: 1119–1122
12 Terauchi H, Cohen J B. Diffuse X-ray scattering due to lattice instability near matal-semiconductor transition in VO_2. Phys Rev B, 1978, 17: 2494–2496
13 Maurer D, Leue A. Elastic behavior near the metal-insulator transition of VO_2. Phys Rev B, 1999, 60: 13249–13252
14 Chen J K, Liu X L. Deoxidization of V_2O_5 powder into VO_2 assisted by an electrochemical lithium intercalation technique. Int J Appl Ceram Technol, 2011, doi: 10.1111/j.1744-7402.2011.00674.x